International Journal of Pharmaceutics, 29 (1986) 195–211
Elsevier

IJP 00981

Fundamentals of release mechanism interpretation in multiparticulate systems: determination of substrate release from single microcapsules and relation between individual and ensemble release kinetics

A. Hoffman [1], M. Donbrow [1], S.T. Gross [2], S. Benita [1] and R. Bahat [1]

[1] *School of Pharmacy, Hebrew University of Jerusalem, Jerusalem 91120 (Israel) and* [2] *Statistics Department, Baruch College, The City University of New York, New York, NY 10010 (U.S.A.)*

(Received May 2nd, 1985)
(Modified version received October 24th, 1985)
(Accepted November 10th, 1985)

Key words: microcapsules – microparticles – release kinetics – release mechanism – parameter distribution statistics – sustained release – controlled release – release single microparticle

Summary

For assessing theories underlying release kinetics of contents from ensembles of microparticles in multiparticle dispersions, population release studies are incapable of revealing the operative physicochemical mechanism, in spite of attempts by many authors to interpret such cumulative data. The present study pioneers techniques for determining release kinetics from single microparticles, using microcapsules as model systems with microconductimetric or spectrophotometric measurement of contents released into the external medium. In four systems giving overall first-order release from populations, the individuals all released their contents at constant rates almost to total payload. A statistical model relating the sum of individual release to cumulative release was applied to the data. It was based on the distribution of two fundamental parameters of the individuals, m_∞ the payload and t_∞ the time to complete release. Statistical analysis of the experimental data validated the proposed relation in the four systems. The conditions required to obtain first-order cumulative kinetics from summated single constant rate data are either: (1) gamma-distribution with shape parameter = 2 of t_∞ and independence of m_∞ and t_∞; or (2) exponential distribution of t_∞ and correlation between m_∞ and t_∞. Cumulative kinetics and rate constants based on an approximation to a standard release equation are useful for characterization of batch release properties (e.g. in checking repeatability, effects of production variables, sustained release character under controlled conditions) but do not reveal the underlying release mechanism or the actual distribution of parameters, which require studies on individuals. Cumulative kinetics may in fact be altered if the distribution profile of the population undergoes accidental or pre-determined change.

Introduction

The purpose of this study is to correlate the release behaviour of populations of small particles with the release of individual particles comprising the ensemble. The study is presented in two parts, designed to facilitate the exposition of the experimental aspects of the work and the theoretical development which followed. The first paper presents the experimental techniques developed in a number of typical systems to study the release of individual particles.

Correspondence: M. Donbrow, School of Pharmacy, Hebrew University of Jerusalem, P.O. Box 12065, Jerusalem 91120, Israel.

Since the individuals prove to observe different kinetics than the populations, a statistical model which determines the cumulative population release from the individual release is developed. Only essential aspects of the model which underlie the analysis of the experimental data are included in the first part. It demonstrates that the data collected on individual particles display the characteristics required by the statistical model to explain the particular ensemble behaviour observed. These results lend experimental support to the adoption of a statistical model as the basis for the development of multiparticulate release kinetics (Hoffman et al., 1985).

The second paper (Gross et al., 1985) presents the detailed statistical treatment for various distributions of individuals and different release mechanisms with particular emphasis on zero-order release from single individuals. It is shown that the various common models of release kinetics can derive purely from the distribution statistics. Later papers will deal with application to forms other than microcapsules.

Among the advantages in using drug-containing microcapsules as models for dissolution in single and multiparticle systems are: the availability for many drugs of simple, sensitive analytical methods for monitoring the low concentrations yielded by single particles in the receiving medium, the existence of preparation techniques enabling formation and isolation of individuals together with good batch reproducibility, and especially, the mathematical simplification entailed in the constancy of particle dimensions throughout the process, i.e. external diameter and wall thickness.

No previous studies on microcapsule release kinetics have been made on individuals (Thies, 1982). The only work on single entities is that of Dappert and Thies (1978a) who carried out a limited study on mass transport into single microcapsules containing aqueous dye solutions as cores based on change in individual capsule characteristics. With methyl orange in the core solution, counts of the numbers of individuals changing colour on penetration of acid from the exterior at fixed times showed the microcapsules to be heterogeneous. Preliminary data were also presented on the change in capsule density with time during extraction, based on the change in terminal velocity of a capsule as it falls through a stagnant liquid column, and appeared to be of too low sensitivity for kinetic treatment. Other methods proposed include the use of cores containing radioactive materials or powerful dyes (Dappert and Thies, 1978b) but their applications are limited. We therefore consider that spectrophotometric, conductometric and similar methods of concentration determination in the extracting medium, as used in the present work, offer a more sensitive approach to kinetic evaluation, adaptable to continuous automated measurement.

The heterogeneous nature of microcapsules prepared by most techniques should not be surprising. Kondo (1978) has drawn attention to the dimensional aspect stating 'the size of microcapsules is never uniform and varies over a fairly wide range'. Other parameters such as surface area, geometric shape, wall thickness, coating porosity and diffusivity have been shown to be important factors determining dissolution rates. However, little is known about distribution profiles of such batch parameters in single particles and it would be anticipated that the variance of the different parameters would be a function of both the microencapsulation technique and the core material size and shape distribution, so that the parameter distributions are not necessarily constant and cannot be taken for granted. This is the essence of the problem of establishing the true mechanism of release from cumulative kinetic data, and it is to this matter that the present series of studies is addressed. Initial consideration will be given to release mechanism and statistical analysis.

Release mechanism: theoretical considerations

In view of the extensive treatments of the well-known equations in the literature, only certain relevant aspects will be quoted here and the main treatments will be applied directly to the data in the Results and Discussion section.

All mass transport rate equations can be derived from Fick's Law, a simple expression of which, for microcapsules, is given by (Dappert and Thies, 1978a):

$$\frac{dm}{dt} = (C_i - C_e)\Gamma \qquad (1)$$

where $C_i - C_e = \Delta c$ represents the concentration difference between the diffusant on the internal (i) and the external (e) sides of the wall membrane, m is mass, t is time and Γ is the capsule wall characteristic, which for a sphere is given by:

$$\Gamma = \frac{4\P D r_i r_e}{r_e - r_i} \quad (2)$$

where D is the diffusion coefficient, and r_i and r_e are the internal and external radii of the microcapsule, the former representing the spherical core radius.

Zero-order release would be expected during constancy of Γ and Δc, so that as long as $C_i = C_s$ (the saturation concentration) and sink conditions prevail ($C_i - C_e \simeq C_i$), this mechanism should prevail. In fact, it is rarely found to hold for batch release, except in the early stages, when it may spuriously fit the initial part of a first-order or other type of curve measured or plotted under less than ideal conditions. Some examples of zero-order (up to a certain degree) have nevertheless been noted (Senjkovic and Jalsenjak, 1981; Jalsenjak et al., 1980; Donbrow and Benita, 1982). In fact, simple calculations reveal a highly significant point to which adequate attention has not been paid, namely, that almost all microencapsulated solids, particularly drugs, should observe constant rate kinetics during the major part of their exit. The percent release P up to which m-t plots should be linear is that at which there is complete dissolution of the diffusant solid core, i.e. the point from which $C_i < C_s$. If the core material has a density of d and V_g is the volume of the solvent needed to dissolve 1g of the core material then:

$$P = 100(V_g d - 1)/V_g \cdot d \quad (3)$$

Table 1 shows some values of P calculated by means of Eqn. 3 for typical core materials, based on literature solubilities and densities. In practice, linearity would extend further, as the curvature would hardly be detectable until at least $C_i \simeq 0.9C_s$. Corrections for the partial specific volume of solute will be required only for very soluble core materials. Since the corrections are relatively small and difficult to estimate, we chose to neglect them at this stage.

TABLE 1

ESTIMATED PERCENT RELEASE (P) FOR ZERO-ORDER LINEARITY IN TYPICAL MICROENCAPSULATED DRUGS

	V_g	d	P
Sodium chloride	2.8	1.75	79.6
Ascorbic acid	3	1.75	79.8
Isoniazid	8	1.4 *	91.1
Paracetamol	70	1.3	98.9
Quinidine sulfate	80	1.44	99.1
Sulfanilamide	100	1.4	99.3
Theophylline	120	1.43	99.4
Aspirin	300	1.4	99.8
Salicylamide	500	1.33	99.9

* Assumed value.

Assuming the solubility of the core material to be unchanged under the conditions of release (i.e. no physical or chemical reactions occur influencing the solubility of the solute core) and also that sink conditions prevail, most drugs should maintain constant rate to approximately 95% release and most salts of moderate solubility to about 80%. We should therefore have expected zero-order behaviour to be the most common for microcapsules. Its rarity in the literature will be shown to be the consequence of parameter variation in populations — only when there is complete identity between all single particles will single and ensemble behaviour match perfectly, as may be the case in some systems (Madan et al., 1976; Bala and Vasudevan, 1982). Whenever any parameter such as core content or rate constant has a non-trivial distribution in the ensemble of particles, then zero-order kinetics is masked in the overall release profile which will take on one of the forms discussed later in this work.

The fact that many or most cumulative data reported hitherto fit best into a first-order framework (Thies, 1982; Donbrow and Benita, 1982; Nixon and Walker, 1971; Madan and Shanbhag, 1978; Jenkins and Florence, 1973; Benita and Donbrow, 1982a, b and c) (or for that matter that some may follow other kinetic models) is not relevant to the mechanism of release from single capsules; it is indeed misleading, and one cannot conclude that the individuals are also of the first-order.

Theoretical analysis shows that first-order behaviour in single capsules may occur in three important situations: (a) when the core material is totally dissolved and the concentration C_i decreases continuously (see Eqn. 1); (b) when the wall/solvent partition coefficient of the core substance highly favours the wall and then only if there is sufficient of the latter to contain all or a major part of the diffusant; and (c) if sink conditions are not maintained (i.e. C_e changes significantly, Eqn. 1). Gaseous cores will also follow similar kinetics.

Even should systems follow these criteria, conformity of both individual and cumulative measurements with first-order conduct requires, as will be shown in Part II, substantial homogeneity of size, shape, content and wall properties, which is rare but may occur (Madan and Shanbhag, 1978). Moreover, the criteria may readily be checked and are clearly not valid for most of the first-order microcapsule data reported, indicating that the behaviour is distribution-derived and not mechanistically-determined.

Reported release data from multiparticular systems apparently observing the *square-root law* ($Q = kt^{1/2}$) have been taken to be cases of Higuchi's matrix model (Oya Alpar and Walters, 1981; Jun and Lai, 1983; El Samaligy and Rohdewald, 1983), applicable to certain drug dispersions in polymer or similar matrices. However, this model must be erroneous for a single microcapsule of classical form, i.e. having a discrete wall and core region. The requirements for matrix behaviour are: erosion of the solute fraction present in excess of its solubility from successive layers of the matrix, with the regressive front extending the thickness of the diffusion layer continuously; further, the dispersed solute particles have to be smaller than the diffusional path. These conditions may conceivably occur in agglomerates of core particles and precipitated wall polymer particles which have failed to coat the cores, the result of unsuccessful microcapsulation technologies, but often undetected if the product is comminuted or forced through a sieve. The error in terming such preparations "microcapsules" has already been pointed out (Benita and Donbrow, 1982a), though individual micropheres meeting the requirements for matrix erosion may theoretically follow the square-root law.

In any event, summation of single particle data observing matrix release kinetics will not give cumulative square-root law kinetics if there is a distribution of parameters among the particles, for the reasons explained earlier and treated in Part II; if cumulative data in fact approximate best to matrix release, an unusual distribution profile is to be expected.

Finally, where release is governed by dissolution rate, whether of uncoated particles or, in microcapsules, of the core material, a cube-root law such as that of Hixson and Crowell (1931) is considered to hold, based on surface area reduction of the dissolving core:

$$W_t^{1/3} = W_o^{1/3} - kt$$

where W_o, W_t are the weights of the particle or core initially and at time t, respectively, and k a rate constant. Again, agreement of cumulative release data with this model (Benita and Donbrow, 1982c) cannot be taken as proof of the release mechanism, unless there is no variation in particle or core properties governing the mathematical form. Langenbucher's dissolution model (Langenbucher, 1969) is subject to the same limitations and is additionally applicable only to homogeneous particles; it was used for microcapsule release studies by Madan (Madan et al., 1976; Madan, 1980).

Wagner's use of probability type of plot (Wagner, 1969) was applied to microcapsules by Nixon and Walker (1971). It is also theoretically unsuitable, being designed for disintegrating-dissolving tablets undergoing surface area changes approximating to a log normal distribution, whereas intact classic microcapsules maintain a constant surface area for diffusion.

Materials and Methods

Microencapsulation procedures

The microcapsules used were prepared by phase separation using non-solvent addition in the presence of a protective colloid, polyisobutylene

(Donbrow et al., 1983, 1984; Benita et al., 1984; Benita et al., 1985). The wall material was Eudragit RS (Roehm Pharma). Core materials included sodium chloride (Frutarom, Israel), granular sodium citrate dihydrate USP (Mallinckrodt) and theophylline USP) (Merck). The last was recrystallized from hot water and passed through standard sieves to narrow the particle diameter range to between 180 and 250 μm.

Batches of the three core materials were prepared under identical conditions using 16% w/w initial Eudragit and one batch using theophylline with 8% w/w Eudragit to obtain more rapid release.

Sampling procedure

Small random samples were transferred and spread on glass slides. Single microcapsules selected randomly were removed, observed microscopically and drawn to scale before measurement of release.

Release rate determination for single microcapsules

(a) Conductivity. A platinum electrode (Radiometer Type CDC 314) was adapted for continuous flow with a peristaltic pump, used to circulate the release medium at 5 ml/min through the electrode and a beaker containing the microcapsule. 10 or 20 ml of release medium was used, the bulk of which was in the beaker, and measurements were made using a Radiometer Conductivity Meter (Type CDM3C) and continuous recorder. The method was suited to determination of electrolyte core materials and in this work was used for sodium chloride and citrate.

(b) Spectrophotometry. Individual microcapsules were put into 1 cm standard rectangular cells containing 4 ml of release medium and allowed to float on the surface, which was outside the optical beam. This method was suitable for microcapsules of a suitable size and containing a core material giving measurable absorbances over the full release, and was used here for the theophylline batches. With stronger absorbances, a continuous flow system was used with a larger quantity of release medium. Release was recorded continuously using a Pye-Unicam UV-Spectrophotometer at suitable fixed wavelength (for theophylline, 272 nm).

Under these conditions, convection caused fairly rapid mixing even without the flow system, as checked by intermittently applied stirring.

Results and principles of statistical treatment

The statistical models developed by the authors in Part II provide the background theory for the analysis of our data (Gross et al., 1985). The data consists of: (a) experimental global release functions $\hat{M}(t)$ for four types of capsules; and (b) experimental individual release functions $\hat{m}(t)$ for samples of the same four types.

A summary of the physical characteristics of the samples is given in Table 2. The four global plots of the release functions are given in Fig. 1. For the single units, 20, 22, 40 and 42 individual capsule release functions were measured for the four capsule types, respectively. A typical set is given in Fig. 2. Two facts emerge from these plots.

(1) Capsules of types 1, 2 and 4 appear to display almost perfect 'first-order' behaviour (Fig. 1). The global release curve for data set 3 deviates somewhat from exponentiality and suggests an ensemble behaviour different from that of sets 1, 2 and 4 even though its single release functions are very similar to those of the remaining sets. These facts along with the χ^2-values for tests of fit to exponential are given in Table 3.

(2) Single capsule release curves (Fig. 2) appear very nearly constant rate curves, but with a great variation in the content and slope. The break points for estimating t_∞, the waiting time for

TABLE 2

PHYSICAL CHARACTERISTICS AND PARAMETERS OF SAMPLES

Sample no.	Sample size = no. of capsules	Type	Wall *	Shape
1	20	Sodium chloride	16%	cube
2	22	Sodium citrate	16%	sphere
3	40	Theophylline	8%	needle
4	42	Theophylline	16%	needle

* Percent (w/w) of Eudragit RS in the initial polymer solution used in production.

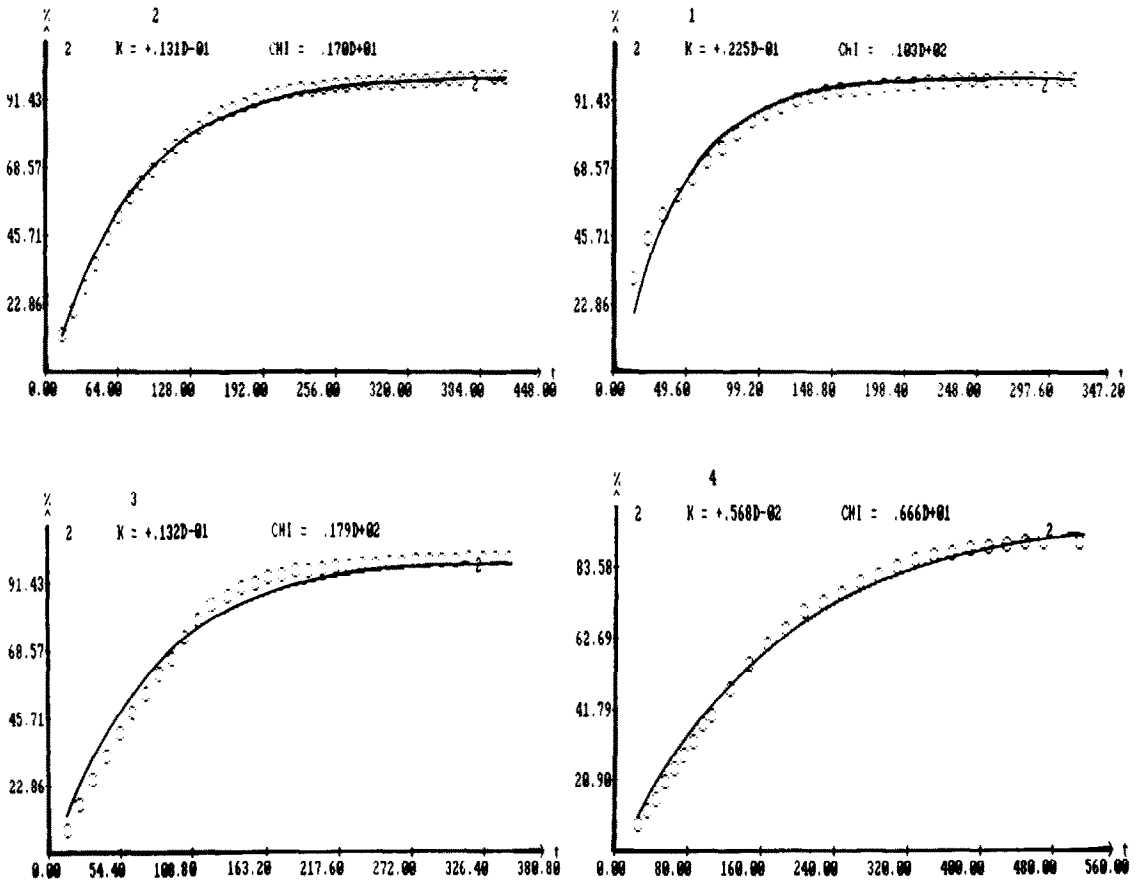

Fig. 1. Global release plots for data sets 1, 2, 3, 4 and their fit to first-order release according to the method described by Benita (1984).

completion of constant rate payload release for a single capsule, were obtained by extrapolation as illustrated in Fig. 2 and Scheme I, in which the maximum height m_∞ is simply the payload of the capsules.

Two theoretical statistical models developed by us (Gross et al., 1985) predict first-order behaviour for ensembles of microcapsules with certain characteristics. We quote them here for comprehensibility. The first set of conditions is: (A) individual

TABLE 3

STATISTICAL FIT OF CUMULATIVE RELEASE TO FIRST-ORDER EQUATION FOR SAMPLES USED

Type	Estimated slope K	Estimated total payload (mg) M_∞	χ^2-test of fit	Degrees of freedom	*P*-value
1	22.5×10^{-3}	1.47	10.3	30	0.9995
2	13.1×10^{-3}	11.60	1.7	39	1
3	13.2×10^{-3}	0.72	17.9	33	0.990
4	5.6×10^{-3}	0.70	6.6	27	1

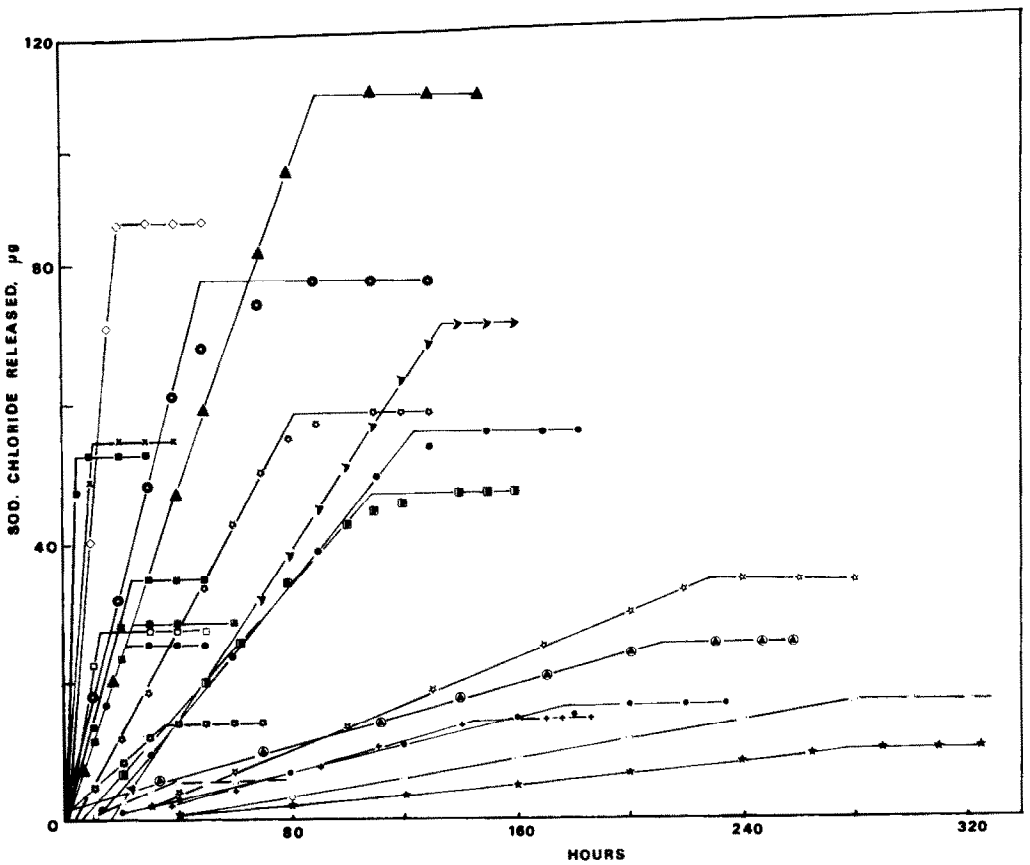

Fig. 2. Individual capsule release curves for microcapsules of sodium chloride (type 1).

capsules release their payload at constant rate so that completion of release is realized at time t_∞, the total payload of a capsule is m_∞ and the constant slope of m(t) is $b = m_\infty/t_\infty$. (B) The distribution of t_∞ in the ensemble of microcapsules is skew-symmetric, i.e. the density of t_∞ tends to have a long right-hand tail. Although most of the capsules will tend to distribute themselves symmetrically about some mean, a few capsules will have disproportionately long release times. Defined mathematically, the density of t_∞ will be gamma with shape parameter $m = 2$ and scale parameter α which will determine the coefficient K of the global exponential release function.

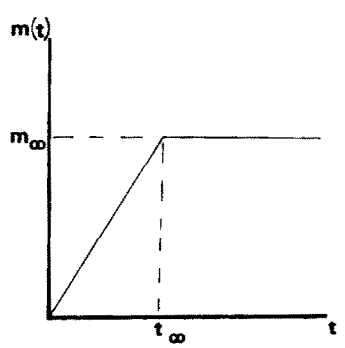

Scheme I

$$M(t) = M_\infty(1 - e^{-Kt})$$

through the relation:

$$K = \alpha$$

The gamma density with parameters m and α has

the form:

$$f(t) = \begin{cases} m!^{-1}\alpha^m t^{m-1} e^{-\alpha t} & \text{if } t > 0 \\ 0 & \text{if } t < 0 \end{cases}$$

(C) The statistical average of m_∞ for all capsules with a given common release time t_∞ does not depend on that common value. If the parameters m_∞ and t_∞ are statistically independent in the population, this condition is certainly satisfied. The condition itself is, however, much weaker than independence and it is satisfied if the conditional mean of m_∞ given any function t_∞, like log (t_∞), is constant in the population.

The second statistical model which leads to first-order release is described by condition (A) above, together with (B′) and (C′) as follows: (B′) the density of t_∞ is exponential or gamma with $m = 1$. (C′) The statistical average of the payload m_∞ for all capsules with a constant release time t_∞ is proportional to that constant value t_∞. In other words, the regression of m_∞ on some function of t_∞ is linear and passes through the origin.

We shall demonstrate through our statistical analysis of the four data sets that the two conditions (B) and (C) are in fact approximately satisfied for data sets 1, 2 and 4. Conditions (B′) and (C′) are approximately satisfied for data set 3. The fit for set 3 is far more imperfect than for the other sets, thus possibly explaining the deviation seen in that case from strict first-order. More specifically, when testing conditions (B′) and (C′) for data set 3, the empirical slope of m_∞ was not found significantly different from zero and the fit of the distribution of t_∞ to the exponential was imperfect.

In the process of validating these conditions in our data, normal probability plots on m_∞ and t_∞ were used and also functions of the same variables like log (m_∞), log (t_∞) and t_∞^θ for fixed values of $\theta > 0$. Our objective was to identify the best transformation of t_∞, $y = g(t_\infty)$ and of m_∞ that would render the transformed variables as nearly normal as possible.

For data sets 1, 2 and 4 the transformation

$$y = \ln(t_\infty)$$

led to an almost perfect normal probability plot thus showing that t_∞ is approximately log-normally distributed. We also found that t_∞ is approximately gamma with shape parameter $m = 2$ in these data sets. In data set 3 the log transformation was less satisfactory, and using gamma and exponential probability plots we concluded that t_∞ is approximately exponential. The normal probability plots for m_∞ and log m_∞ indicated that m_∞ is approximately normal for all four sets although for sets 1 and 2, the fit to a log-normal distribution was better.

For the purpose of carrying out the regression of m_∞ on some function of t_∞ which is approximately normal, $y = \ln(t_\infty)$ was used for data set 1, 2 and 4. For data set 3 we first tried using t_∞ itself for the regression of m_∞ since the relation (C′) we sought predicted $m_\infty(t_\infty)$ to be proportional to t_∞. We also tried $y = \ln(t_\infty)$ and another transformation

$$y = \Phi^{-1}(1 - e^{-\alpha t_\infty})$$

which transforms an exponential variable with scale parameter α and density

$$g(t_\infty) = \alpha e^{-\alpha t_\infty} \qquad \text{if } t_\infty > 0$$

into a standard normal variable. The α used, $\hat{\alpha}$, was estimated from data set 3 by:

$$\hat{\alpha} = \sum_{i=1}^{n} (t_\infty)_i / n$$

which is the customary estimate of the scale parameter of an exponential distribution.

Thus for all four data sets we had a transformation y of t_∞ which could be used in the regression procedure needed to validate conditions (C) or (C′). The regressions were repeated both with m_∞ and log m_∞ where the latter appeared more normal, with identical results. Data will therefore be reported only of the regression of m_∞ on y, which proved to be approximately parallel to the y-axis.

Data analysis

(a) the statistical characteristics of the data

The statistical coefficients for t_∞ and m_∞ for

data sets 1–4 are summarized in Tables 4 and 5, respectively.

Several points may be noted about these data sets.

(i) m_∞ is approximately symmetrically distributed as evidenced by the fact that the sample mean and median are quite close (subject to statistical error), the coefficients of skewness are relatively small (for these small samples) and the sample median is close to the midpoint between the 25% point Q_1 and the 75% point Q_3. Even for data set 3 the skewness of m_∞ is not very marked.

(ii) This is not the case for t_∞ where the right skewness of t_∞ is more marked, especially for data set 3. Notably data sets 1 and 4 display similar degrees of skewness, despite the pronounced difference in their location (mean or median) and variation (standard deviation or range).

(iii) Again noteworthy is the definite skewness of t_∞ in data set 3, which is almost double that of any other data set. This fact indicates that the mild transformation required to transform t_∞ to symmetry, and in fact normality, will probably not suffice entirely for data set 3.

(b) Finding the distribution of t_∞ through transformation and Q–Q plots

In the normal probability plot, quantiles of the (theoretical) Gaussian distribution function:

$$\Phi(t) = \int_{\infty}^{t} 1/\sqrt{\alpha\pi} \cdot e^{-u^2/2} du$$

are plotted against the ordered values of t_∞ in the data. Thus the ith value $t_{(i)}$ is matched with the

$$P_i = (i/n) - \tfrac{1}{2}$$

quantile of the Gaussian distribution. If t_∞ is approximately normal, the Q–Q normal plot results in an approximately straight line (see Chambers, 1977 for details on Q–Q plots as a data analytic tool) whose slope equal $1/\sigma$ and intercept equals $-\mu/\sigma$ where μ and σ denote the mean and standard deviation of the approximate Gaussian distribution for the data. Q–Q normal plots for t_∞ and m_∞ in the four data sets are found in Figs. 3 and 4, respectively. The deviation from a straight line is most marked for data set 3, although for t_∞ the remaining data sets also require transformation to reach linearity. The normal Q–Q plot for the transformed release time $y = \ln(t_\infty)$ appears in Fig. 5.

These plots for sets 1, 2 and 4 appear satisfactorily linear. For data set 3 the right tail of the distribution appears heavier than that of the log-normal distribution, thus causing a turn away from a straight line for large values of t_∞. We conclude that the sets 1, 2, 4 conform to a log-normal distribution and should probably also conform to the gamma distribution with shape parameter $m = 2$ predicted by the statistical theory. This conclusion was in fact validated by the gamma ($m = 2$) Q–Q plots for these data sets found in Fig. 6. However, the gamma plot for set 3 showed distinct departure from gamma with shape parameter 2. The gamma distribution that best fits the data 3 was the exponential. The exponential plot is shown in Fig. 7.

If we compare Fig. 7 with the normal plot for $\ln(t_\infty)$ for data set 3 in Fig. 5, we note that neither the exponential nor the log-normal succeed in fitting both the right and left hand tail of the distribution at once. However, the exponential appears more linear. The distributions fitted to the data are summarized in Table 6.

The normal Q–Q plots for $\ln(m_\infty)$ are shown in Fig. 5B. Possible improvements in linearity over Fig. 4 are evident only in data sets 3 and 4 and they are not very marked. We conclude that m_∞ is normally distributed in sets 1 and 2 and probably log-normally in sets 3 and 4.

(c) The regression of m_∞ on the transformed release time t_∞

The regressions of m_∞ on the $\ln t_\infty$ are approximately valid since both dependent variable (m_∞) and independent variable ($y = \ln t_\infty$) are approximately normal. Since normality of $\ln t_\infty$ is questionable, we also carried out the regression procedure of m_∞ on the variable $y_e = \Phi^{-1}(1 - e^{-\hat{\alpha} t_\infty})$ where $\hat{\alpha}$ was determined from the data (Table 6) $\hat{\alpha} = 6.375 \times 10^{-3}$. Here Φ^{-1} is the inverse of the cumulative of the standard Gaussian distribution given in (b) of this section. This transformation yields a normal variable y

TABLE 4

STATISTICAL MEASURES FOR RELEASE TIMES t_∞

Data set no.	Mean of t_∞ (min) [a]	Standard deviation	Range of t_∞	Coefficient [b] of skewness	Median [c]	Q_1 [d]	(Q_3) [e]
1	182.40 ± 26.14	116.90	12–426	0.66	152 ± 23.1	91.5	231.5
2	100.59 ± 19.21	90.09	6–290	0.78	81 ± 31.8	23	151
3	156.85 ± 13.73	86.82	30–530	2.20	132 ± 8.9	113.5	173.5
4	286.62 ± 23.76	154.0	50–768	1.15	261 ± 30.6	166	340

[a] Mean ± S.E.M.

[b] The coefficient of skewness is zero for symmetric distribution. Large positive values indicate long right-hand tails of the underlying distribution.

[c] Median ± S.E. median.

[d] 25% percentile of the data.

[e] 75% percentile of the data.

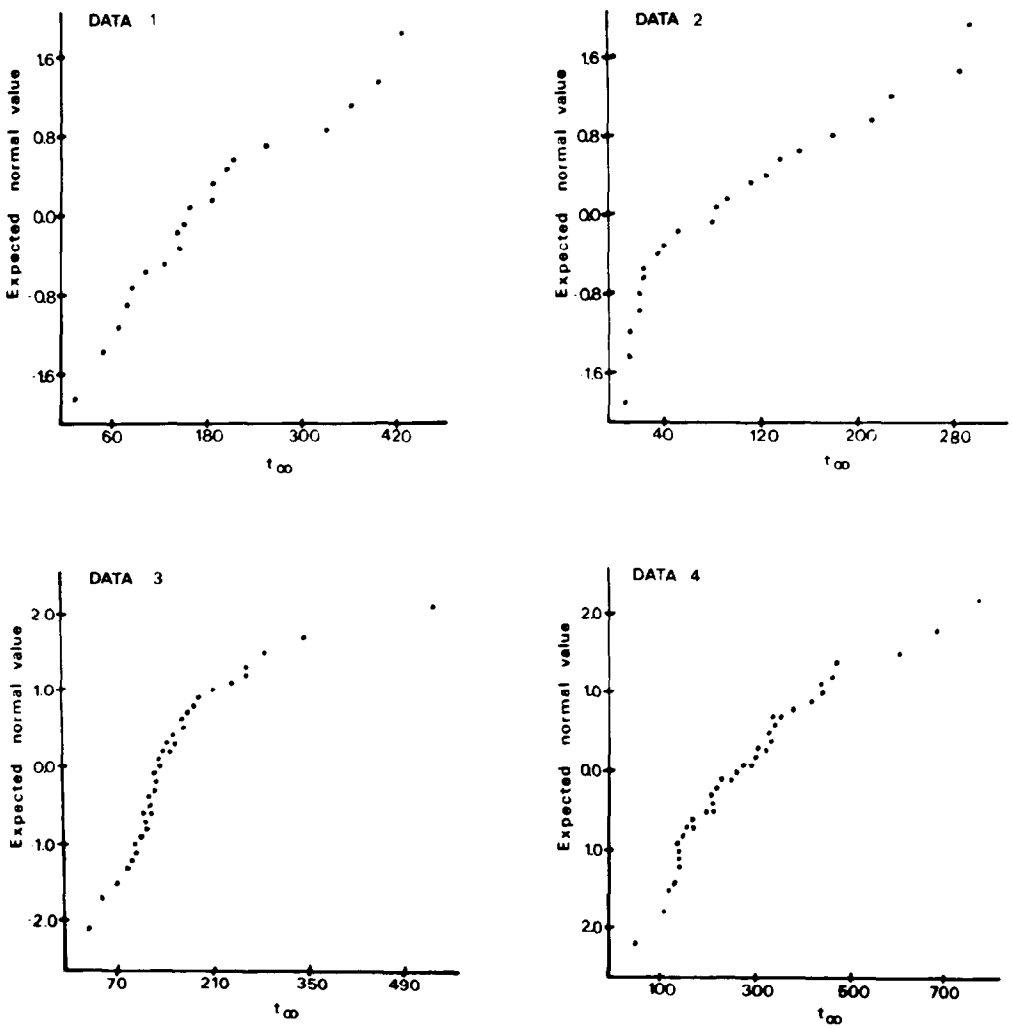

Fig. 3. Q–Q normal plots of t_∞.

TABLE 5

STATISTICAL MEASURES FOR CAPSULE PAYLOAD m_∞

Data set no.	Mean of m_∞ (mg) [a]	Standard deviation	Range of m_∞	Coefficient [b] of skewness	Median of [c] m_∞ (mg)	Q_1 [d]	Q_3 [e]
1	133.7 ±13.72	61.4	8.0–259.0	0.00	145.5 ± 17.9	91.5	175
2	97.9 ±14.73	69.1	8.0–259.0	0.65	78 ±26.6	42	139
3	90.50 ± 7.9	50.0	22.0–276.0	1.28	87.0 ± 10.7	49	114.5
4	83.00 ± 5.26	34.1	27.0–173	0.75	73.5 ± 4.62	56	106

Key as in Table 4.

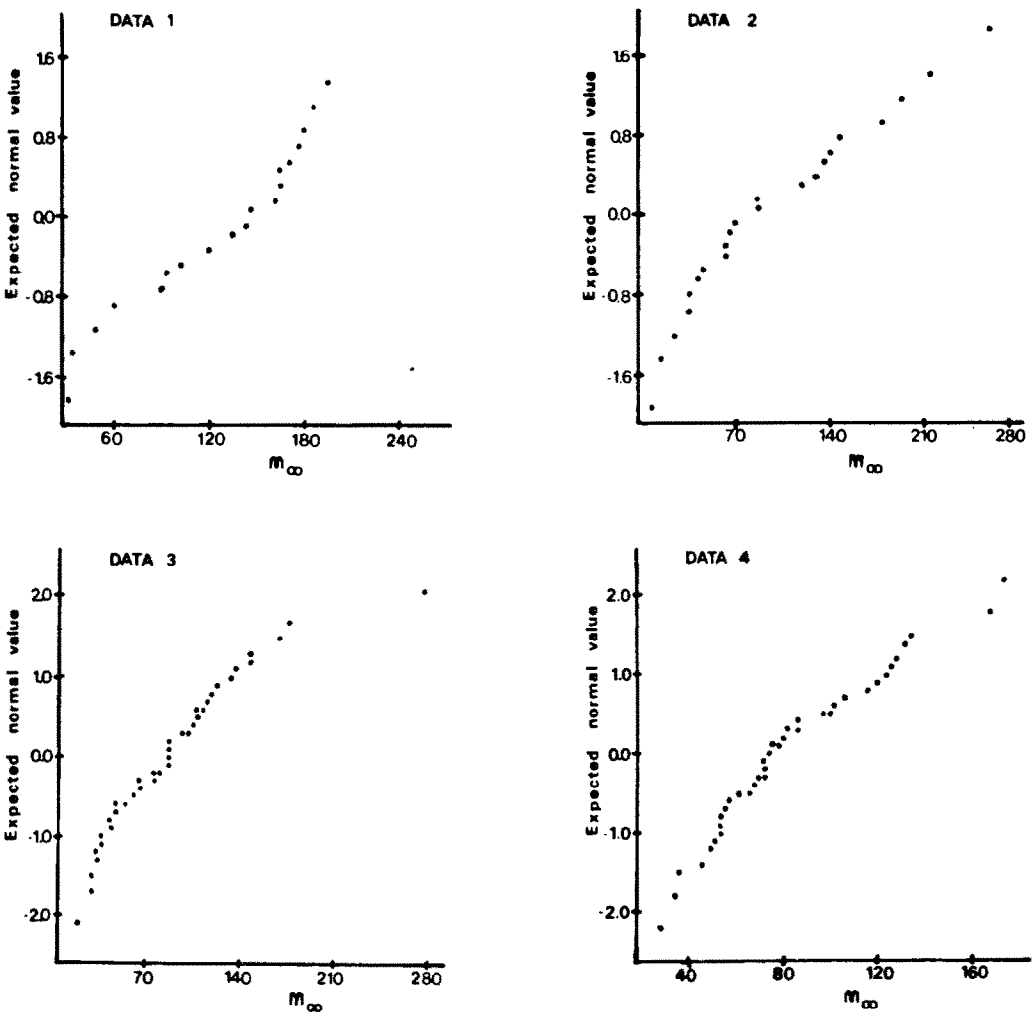

Fig. 4. Q–Q normal plots of m_∞.

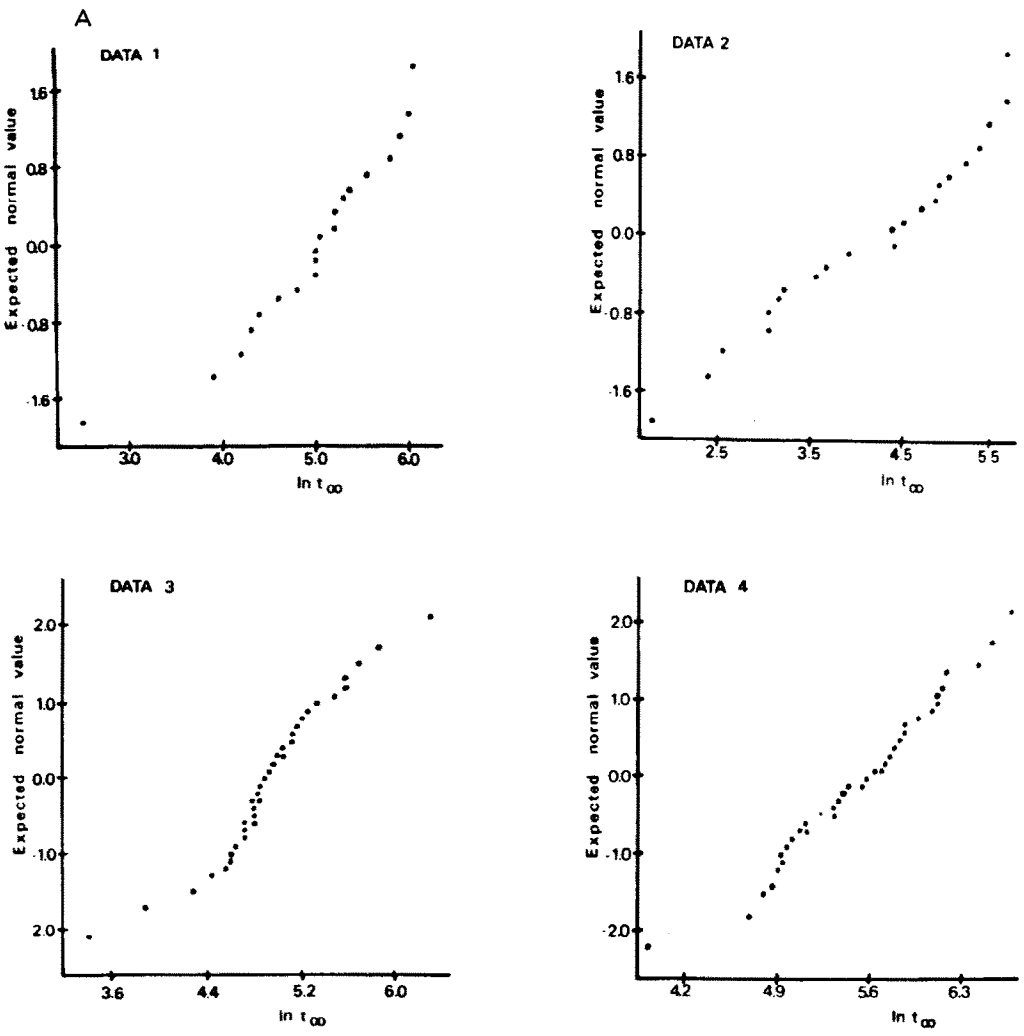

when t is exponential with scale parameter $\hat{\alpha}$. The results are summarized in Table 7. To be noted is the very close agreement in the regression of m_∞ on t_∞, $\ln t_\infty$ and $y_e = \Phi^{-1}(1 - e^{\hat{\alpha} t_\infty})$ for data set 3, as portrayed in Table 7. Regression plots of m_∞ on $\ln t_\infty$ are found in Fig. 8.

The hypothesis that the slope of the regression of m_∞ on a transformed value of t_∞ (which is

TABLE 6

THE FITTED DISTRIBUTION FOR t_∞ ON THE FOUR DATA SETS

Data set no.	Distribution	Alternative distribution	Fit
1	gamma $(2, \alpha = 10.96 \times 10^{-3})$	log-normal $(\mu = 4.9, \sigma = 0.84)$	good
2	gamma $(2, \alpha = 19.88 \times 10^{-3})$	log-normal $(\mu = 4.10, \sigma = 1.14)$	good
3	exponential $(\alpha = 6.375 \times 10^{-3})$	log-normal $(\mu = 4.9, \sigma = 0.50)$	fair
4	gamma $(2, \alpha = 6.98 \times 10^{-3})$	log-normal $(\mu = 5.5, \sigma = 0.54)$	good

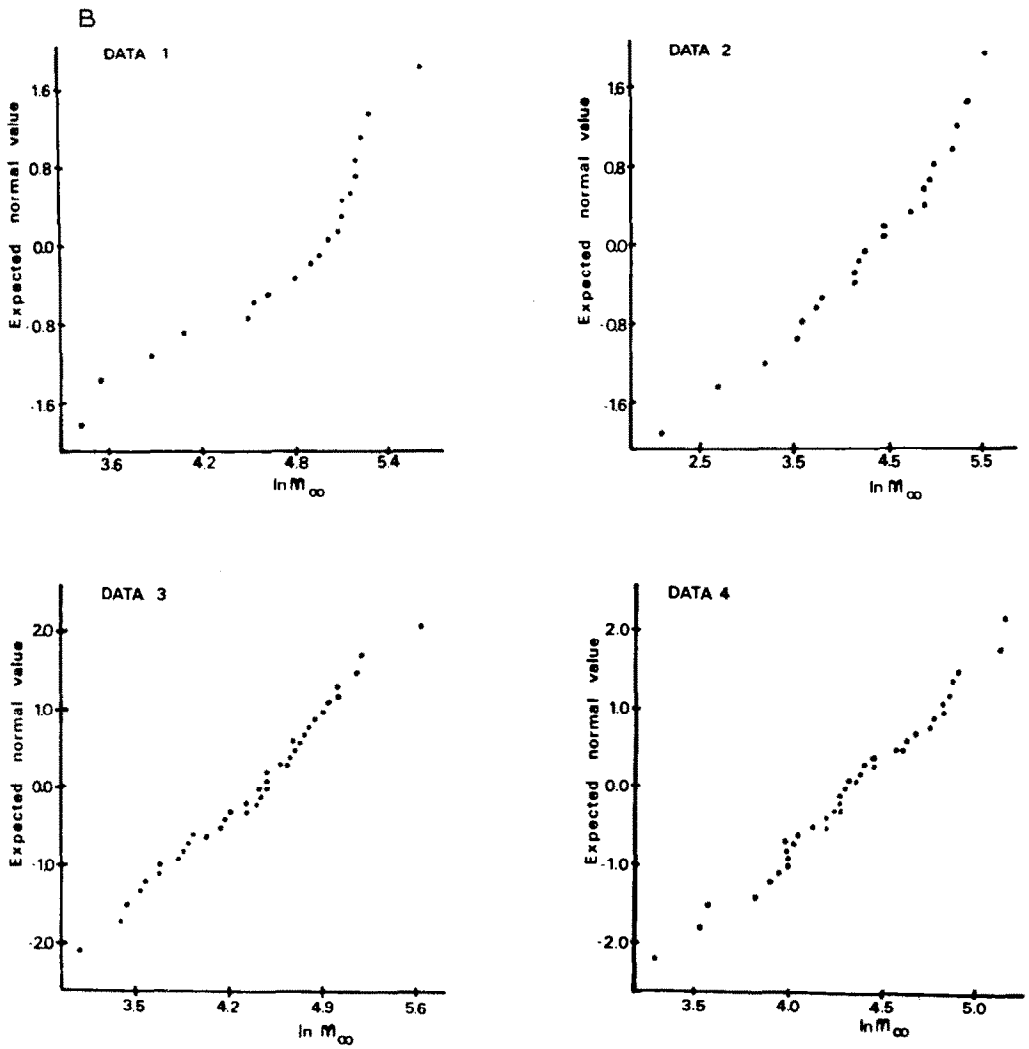

Fig. 5. A: normal Q–Q plots for ln t_∞. B: normal Q–Q plots for ln m_∞.

TABLE 7

REGRESSIONS OF m_∞ ON ln t_∞ FOR DATA SETS 1–4. REGRESSION OF m_∞ ON y_e AND t_∞ FOR DATA SET 3

Data set no.	Dependent variable	Independent variable	Regression slope and intercept	*P*-tail for *F*-ratio	r^2
1	m_∞	ln t_∞	−40.77, 335.68	0.0111	0.31
2	m_∞	ln t_∞	−11.12, 143.54	0.4142	0.03
3	m_∞	ln t_∞	−14.25, 160.82	0.3837	0.02
4	m_∞	ln t_∞	11.19, 21.20	0.2570	0.03
3	m_∞	$y_e = \Phi^{-1}(1 - e^{-\hat{a}t})$	−14.53, 94.25	0.3936	0.02
3	m_∞	t_∞	−0.692, 0.093	0.4597	0.01

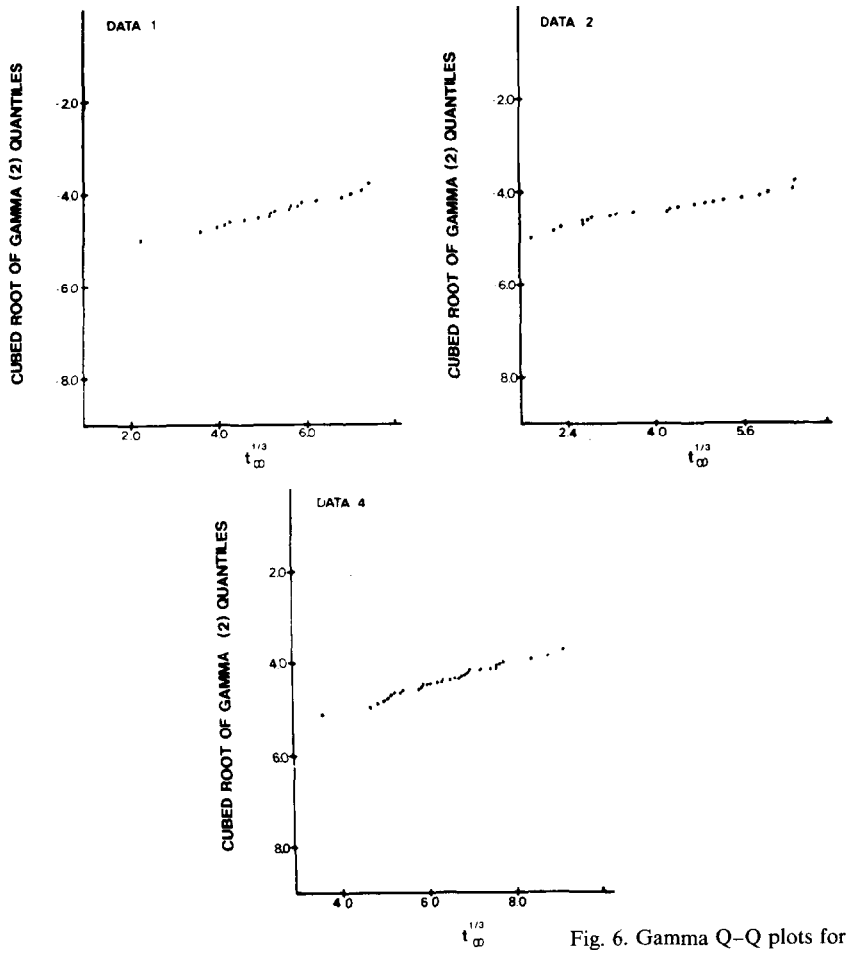

Fig. 6. Gamma Q–Q plots for shape parameter 2. Data sets 1, 2 and 4.

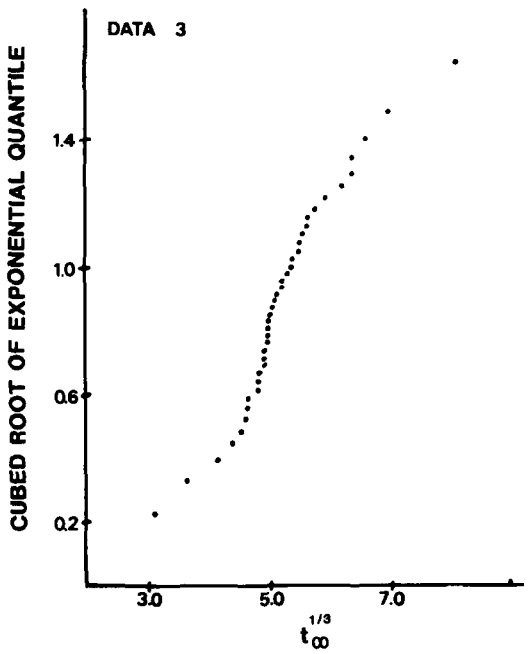

approximately normal) is zero cannot be rejected except for data set 1 where the slope is significantly different from zero. Its r^2 is only 31%, indicating a very weak relation between m_∞ and ln t_∞. The coefficient of determination r^2 measures the fraction of variation of m_∞ in the population of capsules which is explained by the independent variable ln t_∞. Its range for our data is 2–31%.

For data set 3 we found the distribution of t_∞ to be closer to an exponential than to a gamma with shape parameter $m = 2$. The slope of the linear regression of m_∞ on any of the functions we

←

Fig. 7. Exponential Q–Q plot for data set 3.

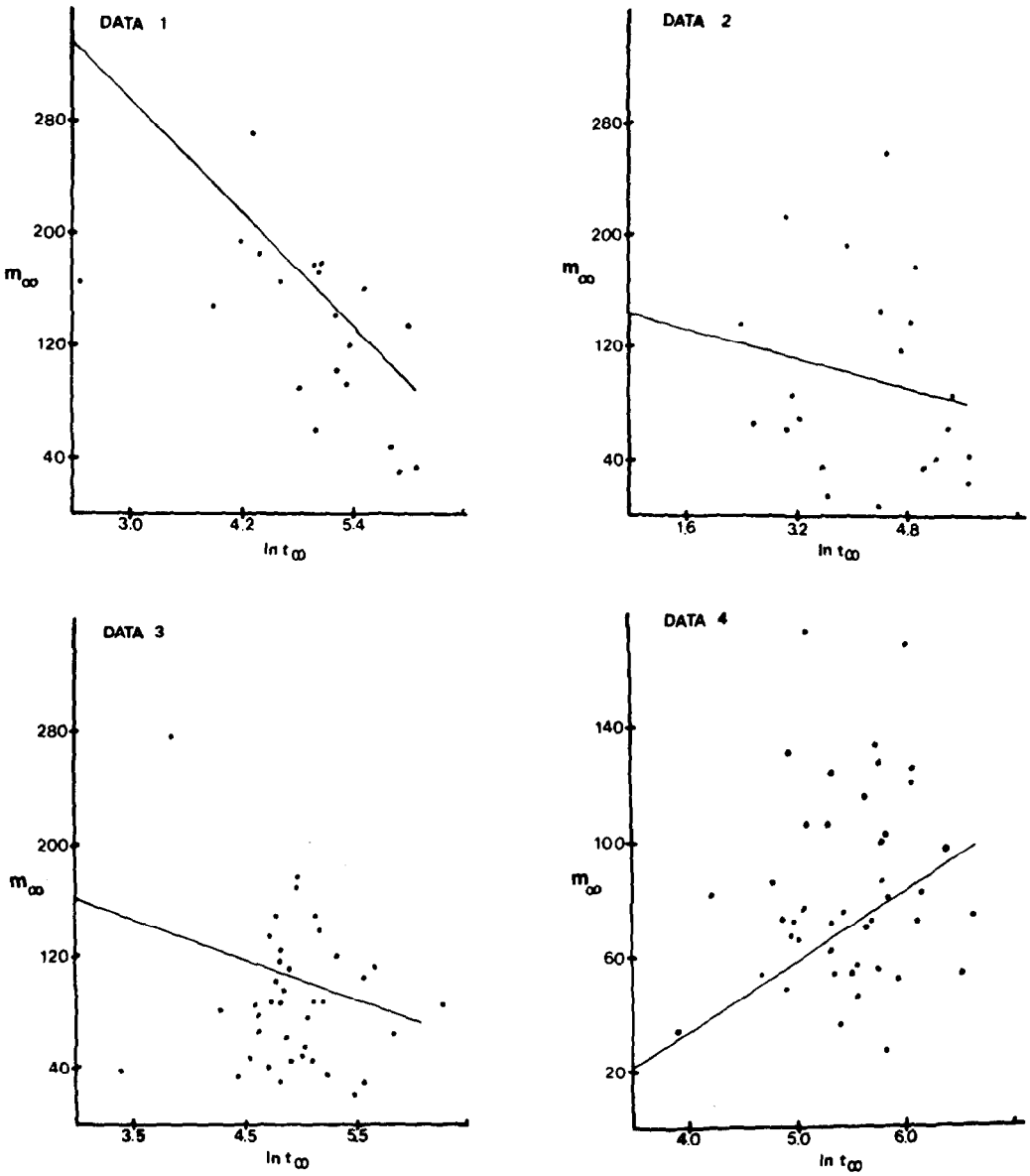

Fig. 8. The linear regression of m_∞ on $\ln(t_\infty)$.

tried, including t_∞ itself, showed lack of correlation between m_∞ and t_∞. Thus neither one of the two models leading to first-order global behaviour appeared to fit the data. The deviation from both models may explain the relatively poor fit of M(t) to the exponential curve.

Conclusions

(1) Release of core material from single microcapsules was measured by physicochemical methods from a large number of individuals. Constant release rate kinetics was universal throughout four

different sets of experiments, cores of high and low solubility being included. Theoretical analysis substantiated this mechanism as being the normal one for microcapsules of classic structure. However, the rate constants and payloads varied greatly between individuals within each set.

(2) Representative ensembles from each set exhibited first-order release behaviour for the population.

(3) Using both graphic and analytic statistical methods we have shown that our data sets largely conform to the statistical model which explains first-order behaviour of an ensemble of microcapsules releasing their payload at constant rate. Data set 3 deviated to some extent from the model, the ensemble fit to first-order release being less exact than in the others; the source of this abnormal behaviour requires further theoretical work.

(4) Deductions of the true mechanism can be made only by micro-investigation of release from single individuals, as in this work. Taken in conjunction with measurements of distribution of particle parameters such as rate constant and content or size, a complete profile can be built up enabling prediction of cumulative release behaviour.

(5) Where cumulative release data are treated by approximation to a standard release equation, for characterization of batch release properties or mean parameters (e.g. for checking repeatability, effects of production and release medium variables, agitation rate, etc.), the picture given of overall release behaviour is not indicative of true release mechanism.

(6) The kinetic form of the cumulative release may be altered when the distribution profile of the population changes or is deliberately changed.

Acknowledgements

The authors would like to acknowledge the support given by Röhm Pharma., F.R.G. This work forms part of the Ph.D thesis of A.H. S.T.G. would like to thank the Hebrew University, Department of Statistics for its generous hospitality during the preparation of this paper.

References

Bala, K. and Vasudevan, P., pH-sensitive microcapsules for drug release. J. Pharm. Sci., 71 (1982) 960–962.

Benita, S., Kinetic model identification from microcapsules using the non-linear regression search procedure. Appl. Biochem. Biotechnol., 10 (1984) 255–258.

Benita S. and Donbrow, M., Effect of polyisobutylene on ethyl cellulose-walled microcapsules: wall structure and thickness of salicylamide and theophylline microcapsules. J. Pharm. Sci., 71 (1982a) 205–210.

Benita, S. and Donbrow, M., Release kinetics of sparingly soluble drugs from ethyl cellulose-walled microcapsules: theophylline microcapsules. J. Pharm. Pharmacol., 34 (1982b) 77–82.

Benita, S. and Donbrow, M., Dissolution rate control of the release kinetics of water-soluble compounds from ethyl cellulose film type microcapsules. Int. J. Pharm., 12 (1982c) 251–264.

Benita, S., Hoffman, A. and Donbrow, M., Non-solvent mixing method of microencapsulation, Israel Patent, No. 63714 (1984).

Benita, S., Hoffman, A. and Donbrow, M., Microencapsulation of paracetamol using polyacrylate resins (Eudragit Retard), kinetics of drug release and evaluation of kinetic model. J. Pharm. Pharmacol., 37 (1985) 341–345.

Chambers, J.M., Computational Methods for Data Analysis, Wiley, New York, NY, 1977.

Dappert, T. and Thies, C., The heterogenous nature of microcapsules, Proc. 5th Int. Symp. Controlled Release of Bioactive Materials, University of Akron, Akron, OH, 1978a, pp. 2.18–2.24.

Dappert, T. and Thies, C., Statistical models for controlled release microcapsules: rationale and theory, J. Membrane Sci., 4 (1978b) 99–113.

Donbrow, M. and Benita S., Release kinetics of sparingly soluble drugs from ethyl cellulose-walled microcapsules: salicylamide microcapsules. J. Pharm. Pharmacol., 34 (1982) 547–551.

Donbrow, M., Benita, S. and Hoffman, A., Production of microcapsules, Israel Patent Application, No. 48788 (1983).

Donbrow, M., Benita, S. and Hoffman, A., Microencapsulation of dichromate and paracetamol with Eudragit Retard Polymers using phase separation by non-solvent addition, Appl. Biochem. Biotechnol. 10 (1984) 245–249.

El Samaligy, M. and Rohdewald, P., Polyacrylamide microbeads, a sustained release drug delivery system. Int. J. Pharm., 13 (1983) 23–34.

Gross, S.T., Hoffman, A., Donbrow, M. and Benita, S., Fundamentals of release mechanism interpretation in multiparticulate systems: the prediction of the commonly observed release equations from statistical population models for particle ensembles. Int. J. Pharm., 29 (1986) 213–222.

Hixson, A.W. and Crowell, Dependence of reaction velocity upon surface and agitation. I Theoretical considerations, Ind. Eng. Chem., 23 (1931) 923–931.

Hoffman, A., Donbrow, M., Gross, S.T. and Benita, S., Correlation of individual and global release profiles from microcapsules. In Peppas, N.A. and Haluska, R.J. (Eds.), Proc. 12th Int. Symp. Controlled Release of Bioactive Materials, Geneva, Switzerland, (1985) 243–244.

Jalsenjak, I., Nixon, J.R., Senjkovic, R. and Stivic, I., Sustained release dosage forms of microcapsulated Isoniazide. J. Pharm Pharmacol., 32 (1980) 678–680.

Jenkins, A.W. and Florence, A.T., Scanning electron microscopy of nylon microcapsules. J. Pharm. Pharmacol., Suppl. 25 (1973) 57–61.

Jun, H.W. and Lai, J.W., Preparation and in vitro dissolution tests of egg albumin microcapsules of nitrofurantoin. Int. J. Pharm. 16 (1983) 65–77.

Kondo, T., Microcapsules: their preparation and Properties in Surface and Colloid Science, Vol. 10, E. Matijevic (Ed.), Plenum, New York, 1978, pp. 1–43.

Langenbucher, F., In vitro assessment of dissolution kinetics: description and evaluation of column-type method. J. Pharm. Sci., 58 (1969) 1265–1272.

Madan, P.L., Clofibrate microcapsules: III Mechanism of release. Drug Devel. Ind. Pharm., 6 (1980) 629–644.

Madan, P.L., Madan, D.K. and Price, J.L., Clofibrate microcapsules: preparation and release rate studies. J. Pharm. Sci., 65 (1976) 1476–1479.

Madan, P.L. and Shanbhag, S.R., Cellulose acetate phthalate microcapsules: method of preparation. J. Pharm. Pharmacol., 30 (1978) 65–67.

Nixon, J.R. and Walker, S.E., The in vitro evaluation of gelatin coacervate microcapsules, J. Pharm. Pharmacol., Suppl. 23 (1971) 147–155.

Oya Alpar, H. and Walters, V., The prolongation of the in vitro dissolution of a soluble drug (phenethicillin potassium) by microencapsulation with ethyl cellulose. J. Pharm. Pharmacol., 23 (1981) 410–422.

Senjkovic, R. and Jalsenjak, I., Surface topography of microcapsules and drug release. J. Pharm. Pharmacol., 33 (1981) 665–666.

Thies, C., Microcapsules as drug delivery devices. Crit. Rev. Biomed. Eng., 8 (1982) 335–338.

Wagner, J.G., Interpretation of percent dissolved – time plots derived from in vitro testing of conventional tables and capsules. J. Pharm. Sci. 58 (1969) 1253–1257.